HHS Public Access

Author manuscript

Schizophr Res. Author manuscript; available in PMC 2022 July 01.

Published in final edited form as:

Schizophr Res. 2021 July ; 233: 101–110. doi:10.1016/j.schres.2021.06.013.

Lower functional connectivity of white matter during rest and working memory tasks is associated with cognitive impairments in schizophrenia

Yurui Gao[1,2], **Muwei Li**[1,3], **Anna S. Huang**[4], **Adam W. Anderson**[1,2,3], **Zhaohua Ding**[1,2,5], **Stephan H. Heckers**[3,4], **Neil D. Woodward**[4,*], **John C. Gore**[1,2,3,*]

[1]Institute of Imaging Science, Vanderbilt University Medical Center, Nashville, TN, USA

[2]Biomedical Engineering, Vanderbilt University, Nashville, TN, USA

[3]Radiology and Radiological Sciences, Vanderbilt University Medical Center, Nashville, TN, USA

[4]Psychiatry and Behavioral Sciences, Vanderbilt University Medical Center, Nashville, TN, USA

[5]Electrical Engineering and Computer Science, Vanderbilt University, Nashville, TN, USA

Abstract

BACKGROUND: Schizophrenia can be understood as a disturbance of functional connections within brain networks. However, functional alterations that involve white matter (WM) specifically, or their cognitive correlates, have seldomly been investigated, especially during tasks.

METHODS: Resting state and task fMRI images were acquired on 84 patients and 67 controls. Functional connectivities (FC) between 46 WM bundles and 82 cortical regions were compared between the groups under two conditions (i.e., resting state and during working memory retention period). The FC density of each WM bundle was then compared between groups. Associations of FC with cognitive scores were evaluated.

RESULTS: FC measures were lower in schizophrenia relative to controls for external capsule, cingulum (cingulate and hippocampus), uncinate fasciculus, as well as corpus callosum (genu and body) under the rest or the task condition, and were higher in the posterior corona radiata and posterior thalamic radiation during the task condition. FC for specific WM bundles was correlated with cognitive performance assessed by working memory and processing speed metrics.

CONCLUSIONS: The findings suggest that the functional abnormalities in patients' WM are heterogeneous, possibly reflecting several underlying mechanisms such as structural damage, functional compensation and excessive effort on task, and that WM FC disruption may contribute

*corresponding authorship.

Credit Author Statement

JCG, NDW and SHH conceived the study design, supervised the project and reviewed the manuscript. YG, ZD and AWA contributed to methodology. YG performed the formal analysis and wrote the manuscript. ML contributed in data preprocessing. ASH prepared data and edited the manuscript.

Declarations of interest: none

to the impairments of working memory and processing speed. This is the first report on WM FC abnormalities in schizophrenia relative to controls and their cognitive associates during both rest and task and highlights the need to consider WM functions as components of brain functional networks in schizophrenia.

Keywords

resting-state fMRI; spatial working memory task; functional connectivity; white matter; cognitive associate

1. Introduction

Schizophrenia, a disorder characterized by cognitive impairments (Blanchard and Neale, 1994; Heinrichs and Zakzanis, 1998; Lee and Park, 2005) Blanchard and Neale, 1994), can be understood as abnormalities of connectivities within neural system (Andreasen et al., 1999; Friston and Frith, 1995). This understanding is supported by neuroimaging studies showing disturbed functional synchronizations between gray matter (GM) regions in schizophrenia and their links to cognitive impairments, in particular within fronto-temporal (Lawrie et al., 2002), fronto-parietal (Kim et al., 2003; Venkataraman et al., 2012), fronto-hippocampal (Meyer-Lindenberg et al., 2005) and thalamo-cortical (Andreasen et al., 1998; Woodward and Heckers, 2016) circuits.

White matter (WM), another fundamental component of the neural system, is the conduit conveying neural signals between GM regions. Pathological changes in WM have been found in patients with schizophrenia, such as dysfunction of myelin sheath lamellae (Davis et al., 2003; Miyakawa et al., 1972), decreases in WM integrity (Ardekani et al., 2003; Kubicki et al., 2003; Nestor et al., 2004; Park et al., 2003), and WM atrophy (Christensen et al., 2004; Haijma et al., 2013; Paillère-Martinot et al., 2001; Sigmundsson et al., 2001), which may undermine the fidelity of neural transmission between WM and GM. We therefore postulated that the functional connectivity (FC) between WM and GM may be disturbed in schizophrenia.

Unlike the FC between GM regions that have been extensively reported in neuroimaging studies, FC involving WM has been largely ignored (Logothetis and Wandell, 2004) partly because there are weaker blood-oxygenation-level-dependent (BOLD) fluctuations expected in WM where much lower blood flow and volume have been found (Helenius et al., 2003). However, emerging evidence has demonstrated that BOLD effects in WM are robustly detectable (Gawryluk et al., 2014; Gore et al., 2019; Li et al., 2019; Mazerolle et al., 2013; Wu et al., 2016), and resting state BOLD signals in WM bundles correlate with those in GM regions to which the bundles connect (Ding et al., 2018; Li et al., 2020; Wu et al., 2019), revealing an apparent functional synchronization between WM and GM. Measurements of FC between WM and GM have been applied to investigate functional alterations in various brain diseases (Bu et al., 2020; Cui et al., 2021; Gao et al., 2020; Ji et al., 2019; Lin et al., 2020). With regard to schizophrenia, a few studies have revealed FC disruption in schizophrenia in WM bundles (Yang et al., 2020) or subnetworks (Fan et al., 2020). However, those studies were limited to an Asian population in a resting state only.

Deficits in working memory, defined as the temporary retention of information in response to immediate information processing demands (Baddeley, 1992), are considered a central cognitive impairment in schizophrenia (Lett et al., 2014). FMRI scans during working memory tasks, in which regional BOLD effects increase in response to the task-induced neural activation, are able to highlight memory-related hypoactive GM regions in schizophrenia (Huang et al., 2019; Manoach et al., 1999). Our previous study found that visual stimuli modulate FC between WM and GM regions within visual circuits in healthy subjects (Ding et al., 2018), but there have been no previous studies reporting whether and how correlations between WM and GM BOLD signals differ in a working memory task between subjects with schizophrenia and normal cognition. Given this background, we hypothesized that FC involving WM, whether during rest or a working memory task, would be altered in schizophrenia and be associated with cognitive functions. Accordingly, in this study we extend our previous analyses (Ding et al., 2018; Gao et al., 2020, 2019) to a cohort of patients with schizophrenia and cognitively healthy controls, quantlifying correlations between BOLD signals during a resting state and during a spatial working memory task. Our specific goals were to: (1) characterize the alterations of FC between WM and GM regions in schizophrenia relative to cognitively normal subjects under rest and task conditions; (2) explore associations between FC of WM and cognitive functions across the cohort.

2. Methods

2.1. Participants

Sixty-seven healthy controls (CON) and 84 patients with schizophrenia spectrum disorders (SCZ) (Table 1) were recruited at Vanderbilt Psychiatric Hospital. The SCZ patients included individuals diagnosed with schizophrenia (n=51), schizoaffective disorder (n=10) and schizophreniform disorder (n=23). The Structured Clinical Interview for DSM-IV Disorders (First et al., 2008) was administered to confirm diagnoses in patients and rule out current or past psychiatric illnesses in healthy participants. Patients were further assessed with the Positive and Negative Syndrome Scale (PANSS) (Kay et al., 1987) to quantify severity of clinical symptoms. Study procedures and exclusion criteria are described in detail in Supplementary material. This study was approved by the Vanderbilt University Institutional Review Board and all participants provided written informed consent.

2.2. Cognitive Assessments

Each participant was administered the same cognitive tests as follows. The Wechsler Test of Adult Reading (WTAR; (Venegas and Clark, 2011)), a single word-reading test, was performed to estimate premorbid intellect. The spatial span and letter-number sequencing subtests from Wechsler Memory Scale-3rd edition (WMS-III; (Wechsler, 1945)) were completed and together yielded the working memory index. The administered Screen for Cognitive Impairment in Psychiatry (SCIP; (Tourjman et al., 2019)) included a word list learning test of verbal memory, a version of the auditory consonant trigrams test of working memory, phonemic verbal fluency and a coding test of processing speed. SCIP subtests raw scores were converted to z-scores and averaged to create a global cognition z-score. The AX Continuous Performance Task (AX-CPT; (Rosvold et al., 1956)) was administered and the d-prime (d'), referred to as d'-context, was computed from the AX hits and BX false alarm

(Cohen et al., 1999). In addition, the Wisconsin Card Sorting Test (WCST; (Grant and Berg, 1948)), a test of executive function, was scored. All the cognitive assessment scores acquired in this study are listed in Table 1.

2.3. Spatial Working Memory Task

Each task fMRI scan comprised 5 spatial working memory trials and 3 non-memory-related trials (Fig. 1A). Subjects were instructed to remember positions of three spatial locations in the memory trial and performed a sensorimotor task without memory requirements in the non-memory-related trial. Each trial started with a 4-second fixation, followed by three dots appearing sequentially within the next 3.5 seconds. After a 16-second retention period, a probe stimulus of 1 second appeared, and the subjects responded to a probe location with a button press indicating whether this stimulus was at one of the three memorized locations. At the end of each trial, there was an inter-trial interval of 13.5 seconds that included the response to the stimulus (Fig. 1B). The non-memory-related trial was identical except that the subjects were instructed not to remember anything but simply to press both buttons when the probe appeared. Different colored dots were used to cue subjects to working memory trial (red dots) or non-memory trial (grey dots). More details were described in a previous study (Huang et al., 2019). The total correct number and total response time were recorded to measure performance of this spatial working memory task, as listed in Table 1.

2.4. MRI Image Acquisition and Preprocessing

One resting state fMRI scan (sequence=gradient-echo echo-planar imaging, TR/TE=2s/35ms, resolution=3×3×3 mm^3, matrix=80×80×38, dynamic volumes per scan=300, eyes closed), six working-memory task fMRI scans (same parameters except dynamics per scan=152) and one T1-weighted scan (sequence=turbo field echo, TR/TE=8ms/3.7ms, resolution=1×1×1mm^3, matrix=256×256×170) were acquired for each subject using one of two identical 3T MRI scanners (Philips Healthcare Inc., Best, Netherlands) with 32-channel head coils at Vanderbilt University Institute of Imaging Science.

Image preprocessing is described in detail in Supplementary material. Briefly, preprocessing of fMRI images included correcting slice timing and head motion, regressing out 24 motion parameters and mean cerebrospinal fluid (CSF) signal, temporal filtering (passband=0.01–0.1Hz), co-registering to the Montreal Neurological Institute (MNI) space, detrending, and voxel-wise normalization of the time-courses into zero mean and unit variance. In order to avoid signal contamination between WM and GM in preprocessing, we did not spatially smooth fMRI data. Preprocessing of T1-weighted images included segmenting WM, GM, and CSF and co-registering the resultant tissue probability maps to the MNI space.

2.5. Analyses of Functional Connectivity between White Matter and Gray Matter

All further analyses in this study were based on calculation of the functional correlation matrix (FCM), which is a matrix of correlations between 46 WM bundles and 82 GM regions of interest (ROIs). The WM bundles and GM ROIs were initially defined by the Eve atlas (Oishi et al., 2009) (20 deep WM bundles in each hemisphere and 6 commissure bundles, shown in Fig. 1C and Table 2) and PickAtlas (Lancaster et al., 2000) (41 Brodmann areas in each hemisphere, shown in Fig. 1D and Table 2), respectively, and were further

constrained within whole-brain WM or GM masks generated by thresholding the WM or GM tissue probability maps at 0.8 (Fig. 1E) in order to avoid partial volume effects. The preprocessed time-courses were spatially averaged over each ROI. The two averaged time-courses from each pair of WM and GM ROIs were then linearly correlated, excluding any frames with large head motions (i.e., frame-wise displacement (Power et al., 2012) >0.5; average number of excluded frames per SCZ subject = 16; average number of excluded frames per CON subject = 9; minimum number of remaining frames per subject = 205). The resulting correlation coefficients comprised an FCM (size: 46×82) of WM-GM pairs. The possible influences of sex, race, age, maternal and paternal years of education were regressed out from the FCM using a general linear model. Fisher's z-transforms were applied to all the correlation coefficients in FCM.

To compare WM-GM FC between SCZ and CON groups, we averaged the FCMs across subjects within each group, denoted as the mean FCM (mFCM; size=46×82), and then subtracted mFCM of the SCZ group from mFCM of the CON group element by element. Meanwhile, an unpaired *t*-test was conducted for each FCM element to determine the significance of the inter-group difference in FC. The resulting *p*-values (n=46×82) were corrected for multiple comparisons using a false discovery rate (FDR) (Benjamini and Hochberg, 1995), denoted as p_{FDR}. The effect size of the difference (Cohen, 2013) for each FCM element between groups was also calculated.

2.6. Analyses of White Matter Functional Connectivity Density

Inspired by the idea of FC density mapping proposed in a previous study (Tomasi and Volkow, 2010), we defined WM FC density as the average FC between one WM bundle and all GM ROIs across the entire cerebral cortex. Specifically, the density for each WM bundle was calculated by averaging the magnitudes of the 82 FCM elements corresponding to this WM bundle. The mean and standard deviation of the WM FC density for each WM bundle across subjects within each group were then computed. The group means were compared using permutation tests (100,000 permutations) with a correction of multiple comparisons $p<(1/N)=(1/46)=0.022$. This correction means that less than one false-positive bundle is expected among all 46 bundles (Lynall et al., 2010).

2.7. Association with Cognitive Scores

The association between each single FCM element, i.e., FC of one WM-GM pair, and each cognitive score was evaluated by calculating the Pearson's correlation coefficient, r, between them across all subjects. The resulting *p*-values (n=46×82) for each score were corrected using FDR. Accordingly, for each score, each WM bundle had 82 correlation coefficients from which the one with maximum amplitude and $p_{FDR}<0.05$, which reflected the strongest and most significant correlation, was selected to represent the association between the WM bundle FC and the score. This association measure is more sensitive to local correlations but may also be less resistant to local noise. Considering this, we report only the non-negligible correlations, i.e., $|r|>0.3$ (Cohen, 2013). Furthermore, the p_{FDR} values of 46 bundles were further corrected for multiple comparisons using $p_{FDR}<(1/46)=0.022$.

2.8. Resting State and Task Conditions

The above analyses were separately performed under resting state and task conditions. Under the resting state condition, each time-course for FCM computation included all eligible frames from the resting state fMRI scans. Under the working memory task condition, each time-course included only the frames acquired during the memory retention periods (8s-24s) in all 30 memory trials (5 trials per scan × 6 scans per subject). For comparison, we also did the same analyses based on the entire time-courses of the working memory task.

3. Results

3.1. Participant Characteristics

Table 1 summarizes the demographic, clinical, and cognitive characteristics of all 151 participants from the CON group (n=67) and SCZ group (n=84). No significant differences in age (p=0.302), sex (p=0.394), race (p=0.063), handedness (p=0.656), maternal education (p=0.874) and paternal education (p=0.571) were observed between the two groups. As anticipated, all the cognitive scores and fMRI task scores were significantly different between the two groups (p<0.010).

3.2. Functional Connectivity between WM and GM

Fig. 2 shows the mFCM of the CON and SCZ groups under two conditions: resting state and retention period during working memory task. The general patterns of mFCM under the two conditions appeared similar at first glance, but significant differences were in FC of some WM-GM pairs between conditions, as shown in Supplementary Fig. 1. Compared to mFCM of the CON group, mFCM of the SCZ group under the same condition appeared to have a generally similar but weaker FC pattern.

The element-wise differences of mFCM between the CON and SCZ groups under rest and task conditions are shown in Fig. 3A and 3C, where only the differences with statistical significance ($p_{FDR} < 0.05$) are presented with non-zero values. Clearly, the SCZ group had lower FC at several WM-GM pairs but also higher FC at a few WM-GM pairs than the CON group under each condition. The effect sizes of the group differences for the elements with $p_{FDR} < 0.05$ were all higher than 0.45 under the two conditions, as shown in Fig. 3B and 3D, indicating that the differences were not trivial.

3.3. White Matter Functional Connectivity Density

A group comparison of the FC density of each WM bundle under each condition is presented in Fig. 4 and Supplementary Table 1. In a resting state (Fig. 4A), FC densities in SCZ relative to CON were significantly lower (p<0.022) in bilateral external capsule (EC; both p<0.001), bilateral cingulum near cingulate gyrus (CGC; p=0.014 and 0.016, respectively), bilateral uncinate fasciculus (UF; p=0.006 and 0.017, respectively), genu of corpus callosum (GCC; p=0.004) and body of the corpus callosum (BCC; p=0.006). In the working memory task condition (Fig. 4B), significant lower FC densities in SCZ relative to CON were found at bilateral EC (p=0.010 and 0.021, respectively), bilateral CGC (p=0.015 and 0.021, respectively) and right cingulum near hippocampus (CGH; p=0.017). Besides,

BCC (p=0.027) and right fornix cres (FXC; p=0.025) exhibited a trend to a significant lower density in SCZ. By contrast, left posterior thalamic radiation (PTR; p=0.013) and right posterior corona radiata (PCR; p=0.012) had significantly higher FC densities in SCZ relative to CON.

3.4. Associations between White Matter Functional Connectivity and Cognitive Scores

The significant and non-negligible associations (thresholding criteria: p_{FDR}<0.022 and |r| >0.3) between FC and cognitive scores are depicted in Fig. 5.

Under a resting state condition (Fig. 5A), positive correlations (p_{FDR}<0.022 and r>0.3) were found between FC and WMS-III working memory index in left EC (r=0.38, p_{FDR}=0.003), bilateral CGC (r=0.36, p_{FDR}=0.003 and r=0.35, p_{FDR}=0.004, respectively), left UF (r=0.39, p_{FDR}=0.003), pontine crossing tract (PCT; r=0.33, p_{FDR}=0.005), right CGH (r=0.38, p_{FDR}=0.002), right posterior limb of internal capsule (PLIC; r=0.32, p_{FDR}=0.007), right anterior limb of internal capsule (ALIC; r=0.33, p_{FDR}=0.006) and right medial lemniscus (ML; r=0.35, p_{FDR}=0.004). Positive correlations were also found between FC and SCIP processing speed in bilateral superior longitudinal fasciculus (SLF; r=0.37, p_{FDR}=0.011 and r=0.35, p_{FDR}=0.019, respectively). Non-negligible correlations were not observed between FC and other cognitive scores including WTAR Premorbid IQ, SCIP verbal learning-immediate/delayed z-score, SCIP working memory z-score, SCIP verbal fluency z-score, SCIP global cognition z-score, AX-CPT d'-context, and WCST total correct score.

Under a working memory task condition (Fig. 5B), WMS-III working memory index was positively correlated (p_{FDR}<0.022 and r>0.3) with FC in middle cerebellar peduncle (MCBP; r=0.37, p_{FDR}=0.010). Meanwhile, the SCIP processing speed was positively correlated with FC at left superior corona radiata (SCR; r=0.31, p_{FDR}=0.017), bilateral CGC (r=0.33, p_{FDR}=0.016 and r=0.36, p_{FDR}=0.010, respectively), bilateral SLF (r=0.33, p_{FDR}=0.020 and r=0.37, p_{FDR}=0.010, respectively), BCC (r=0.35, p_{FDR}=0.016), and right FXC (r=0.32, p_{FDR}=0.017). Non-negligible correlations were not observed between FC and other cognitive scores.

4. Discussion

We evaluated measures of FC within WM bundles, their differences between subjects with schizophrenia and normal cognition, and their correlations with cognitive scores under both resting state and working memory task conditions. We found that 1) FC values between WM and GM ROIs were mainly lower in schizophrenia compared to controls under both conditions, with a few exceptions; 2) WM FC densities were lower in schizophrenia relative to normal in several WM bundles (e.g., long association and commissural bundles) under the two conditions, again with a few exceptions (e.g., parietal projection bundles) in the task condition; and 3) WM-GM FC was non-negligibly associated with measures of cognition including working memory as well as processing speed in both conditions. Together, these findings indicate that FC measures within WM reflect functional abnormalities in schizophrenia and suggest a role for FC alterations within WM in cognitive impairments in schizophrenia.

Although overall patients and controls exhibited a similar pattern of WM-GM FCM during both rest and task (Fig. 2), differences in FC were evident for several WM-GM pairs (Fig. 3). These differences indicate mainly a reduced functional synchronization between WM and GM regions in schizophrenia relative to controls, with some notable exceptions in areas in which controls appear less engaged than patients. WM-GM FCM patterns were very similar between rest and task, convergent with existing evidence showing a strong correlation of GM-GM at rest and during a memory task (Cole et al., 2014), suggesting that rest and task share the same intrinsic networks.

When the brains were at rest, lower WM FC densities in the SCZ group relative to the CON group were detected at long association bundles (i.e., bilateral EC, CGC, and UF) and commissural bundles (i.e., GCC and BCC) (Fig. 4A). Reduced fractional anisotropy (FA), increased radial diffusivity and other microstructural abnormality in schizophrenia in these structures have been repeatedly reported in prior diffusion MRI studies (Koshiyama et al., 2020; Kubicki et al., 2003; Lee et al., 2013; Nestor et al., 2004; Schilling et al., 2018; Skudlarski et al., 2013). The consistency between functional and structural disruptions in these bundles indicates that the disrupted synchronization between the bundles and cerebral cortices in schizophrenia at rest may be partially explained by the structural degradation reported by others in these bundles. By contrast, when there was a working memory demand, lower FC density in right CGH in schizophrenia became apparent (Fig. 4B). Previous lesion studies have directly demonstrated that cingulum participates in working memory functioning (Ennaceur et al., 1997; Gaffan, 1994) and diffusion MRI studies have revealed that FA at CGH decreased in schizophrenia compared to controls (Abdul-Rahman et al., 2011). Additionally, FC values between right CGH and bilateral BA8 areas (frontal eye field; FEF) were lower in schizophrenia during only task (Fig. 1). FEF has been demonstrated to be activated during working memory retention stage (Pessoa et al., 2002; Rottschy et al., 2012) and be hypo-activated in schizophrenia (Driesen et al., 2008; Huang et al., 2019). Combining these findings, the possible explanations for our observed lower FC density in CGH during memory retention may involve structural degradation of the bundle and dysfunction within impaired working memory circuit in schizophrenia. These findings also suggest that adding functional loads to a brain network may increase the chance of observation of FC abnormalities in those WM bundles that are highly engaged in the function. Besides, one recent resting state fMRI study reported lower FC in treated patients relative to controls in GCC, PCT, CGH and CST (Yang et al., 2020), which were a subset of our results from two conditions when using the uncorrected significance level of 0.05.

Interestingly but not surprisingly, PTR and PCR in the SCZ group showed a higher FC density than the CON group during working memory retention. There is literature revealing microstructural damage to PTR and PCR (Koshiyama et al., 2020) and involvement of thalamic dysfunction in working memory deficits in schizophrenia (Eryilmaz et al., 2016). In turn, the hyper-FC density of PCR may be explained by excessive recruitment of local neural circuitry in patients due to inefficiency of neural communication (Ramsey et al., 2002). Alternatively, hyper-FC on PTR may be related to a compensatory mechanism during a task in patients, especially considering that posterior parietal lobe appears to serve for

phonological storage of information (Cohen et al., 1997) and is hyper-activated during working memory tasks (Mendrek et al., 2005).

The FC density calculated from the entire time-course of the working memory task (Supplementary Fig 2E) revealed that ALIC and CP had a tendency to lower FC in schizophrenia relative to controls. The two stages of the task other than memory retention (i.e., encoding and retrieval, Supplementary Fig. 3) may contribute to this result. Comparing the two task conditions (Fig. 3C and Supplementary Fig. 2C), the ALIC-paired GM ROIs with a lower FC only when including the entire time-course included BA5 (superior parietal lobe), BA18/19 (visual cortex V2-V5), BA24 (anterior cingulate cortex) and BA37 (fusiform gyrus), which are more engaged in sensory, attention, decision making and visual recognition than memory retention. Several studies have reported smaller diffusion metrics or volume size of ALIC in schizophrenia (Levitt et al., 2010; Rosenberger et al., 2012; Zhou et al., 2003), although others did not find a consistent result (Levitt et al., 2010; Paillère-Martinot et al., 2001). ALIC contains fibers passing through CP, which may at least in part explain the similarity in alterations of FC density between ALIC and CP (Supplementary Fig. 2C).

The observed associations between FC of WM and cognitive performance (Fig. 5) are supported by other evidence. First, the positive associations with WMS-III working memory index were non-negligible not only in long association bundles (e.g., EC, CGC and UF) and projection bundles (e.g., ALIC and PLIC) in cerebrum during the rest but also in cerebellar bundles (i.e., MCBP) during the task. Previous diffusion MRI studies reveal that the same working memory index or other working memory metrics positively correlated with FA in EC, CGC, UF and ALIC in schizophrenia or Parkinson's disease (Kubicki et al., 2003; Levitt et al., 2010; Nestor et al., 2004; Theilmann et al., 2013), providing a possible structural explanation for the FC-cognition association in cerebrum during the rest. As to cerebellar bundle, accumulating evidence reveals that cerebellar abnormalities in schizophrenia, such as diminished blood flow and impaired synaptic architecture, are linked to deficits in working memory and disturbances of the prefronto-thalamo-cerebellar circuit contribute to the pathophysiology of schizophrenia (Andreasen et al., 1996; Wiser et al., 1998; Yeganeh-Doost et al., 2011). Thus, we may infer that the observed associations with cerebellar bundle may be an extension of the association of cerebellum produced through the prefronto-thalamo-cerebellar circuit. Second, the association with SCIP processing speed, but not with other SCIP sub-functions (verbal learning-immediate/delayed, working memory, verbal fluency, and global cognition), is in accordance with a prior diffusion MRI study showing that degradation of WM integrity is correlated with impairment of processing speed but no other functions measured by SCIP (Karbasforoushan et al., 2015). In particular, the related WM bundles (i.e., SLF, UF, BCC, SCR, CGC and FXC) found in the present study are highly consistent with the findings (i.e. corpus callosum, cingulum, bundles under superior and inferior frontal gyri and precuneus) in the previous diffusion study (Karbasforoushan et al., 2015). To sum up, the above evidence repeatedly suggests that the FC-cognition covariation in WM is consistent with known structure-cognition covariations in WM bundles, and with FC-cognition or structure-cognition covariations in GM engaged in the same circuits.

The measurement of WM-GM FC in our study followed the same methodology that has commonly been used to estimate GM-GM FC, but the interpretation of WM-GM FC remains uncertain. However, the possibility that the WM-GM FC could arise from partial volumes effect (PVE) between WM and GM ROIs was reduced because we skipped spatial smoothing, used the deep WM atlas (Fig. 1C) and applied a highly conservative mask to constrain WM and GM ROIs (Fig. 1E). Another common concern is that the BOLD signal changes observed in WM could arise from neighboring GM by vascular drainage effects, rather than originating from intrinsic processes in WM. However, Millan *et al.* found that the deep venous system draining deoxygenated blood in deep WM is separate from the superficial venous system draining blood in GM and superficial WM (Ruíz et al., 2009), suggesting that BOLD signals in deep WM are unlikely to be affected by vascular changes in GM.

Our investigation has several potential limitations. First, the WM atlas we used here covers the WM bundles primarily deep in the brain, some of which lack the portions extending to the surface. Matched diffusion MRI data and WM tractography will allow us to obtain more accurate WM bundles for individuals in future investigations. Second, one major WM bundle may be comprised of multiple pathways connecting different cortical regions (Schmahmann and Pandya, 2009) and be engaged in different neural activities, so BOLD signals could be inhomogeneous over the WM bundle. In this case, averaging the time-courses over the bundle probably compromised the spatial specificity of the origins of the signal variations. Third, a potential confounding variable for the analyses under task condition could be the task performance, which was different between the CON and SCZ groups (Table 1). Specifically, the decrease of functional connectivity in SCZ relative to CON might due to the worse performance of working memory task in SCZ rather than schizophrenic disorder (Eryilmaz et al., 2016; Rodrigue et al., 2018; Thermenos et al., 2005; Van Snellenberg et al., 2006). Controlling for the task performance might be a solution to rule out this effect but meanwhile might bring overfitting bias because the task performance has been found positively associated with retention-related activations in GM regions using the same data (Huang et al., 2019). Another solution could be selecting only correct trials for FC measurement, but it would reduce the signal to noise ratio.

5. Conclusions

In conclusion, findings from this study indicate that the FC abnormalities in WM may have a heterogenous underlying mechanism and be a contributor to reduced working memory and impaired processing speed in schizophrenia. To the best of our knowledge, this study provides a first evaluation of FC alterations in WM bundles under task conditions in schizophrenia compared to healthy controls and their associations with cognitive functions, highlighting the importance of understanding WM functions as components of brain functional networks in schizophrenia.

Supplementary Material

Refer to Web version on PubMed Central for supplementary material.

Acknowledgments

We thank the Advanced Computing Center for Research and Education (ACCRE) at Vanderbilt University for distributed computation. This work was supported by NIH grants NS093669 and NS113832 (Gore), MH102266 (Woodward), Vanderbilt Discovery Grant FF600670 (Gao), and the Charlotte and Donald Test Fund.

References

Abdul-Rahman MF, Qiu A, Sim K, 2011. Regionally specific white matter disruptions of fornix and cingulum in schizophrenia. PLoS One6, e18652–e18652. doi:10.1371/journal.pone.0018652 [PubMed: 21533181]

Andreasen NC, Nopoulos P, O'Leary DS, Miller DD, Wassink T, Flaum M, 1999. Defining the phenotype of schizophrenia: Cognitive dysmetria and its neural mechanisms. Biol. Psychiatry doi:10.1016/S0006-3223(99)00152-3

Andreasen NC, O'Leary DS, Cizadlo T, Arndt S, Rezai K, Boles Ponto LL, Watkins GL, Hichwa RD, 1996. Schizophrenia and cognitive dysmetria: A positron-emission tomography study of dysfunctional prefrontal-thalamic-cerebellar circuitry. Proc. Natl. Acad. Sci. U. S. A93. doi:10.1073/pnas.93.18.9985

Andreasen NC, Paradiso S, O'Leary DS, 1998. "Cognitive dysmetria" as an integrative theory of schizophrenia: A dysfunction in cortical-subcortical-cerebellar circuitry?Schizophr. Bull doi:10.1093/oxfordjournals.schbul.a033321

Ardekani BA, Nierenberg J, Hoptman MJ, Javitt DC, 2003. Mri study of white matter diffusion anisotropy in schizophrenia. Neuroreport14. doi:10.1097/00001756-200311140-00004

Baddeley A, 1992. Working memory. Science (80-.)255, 556 LP – 559. doi:10.1126/science.1736359

Benjamini Y, Hochberg Y, 1995. Controlling the False Discovery Rate: A Practical and Powerful Approach to Multiple Testing. J. R. Stat. Soc. Ser. B57. doi:10.1111/j.2517-6161.1995.tb02031.x

Blanchard JJ, Neale JM, 1994. The neuropsychological signature of schizophrenia: Generalized or differential deficit?Am. J. Psychiatry151, 40–48. doi:10.1176/ajp.151.1.40 [PubMed: 8267133]

Bu X, Liang K, Lin Q, Gao Y, Qian A, Chen H, Chen W, Wang M, Yang C, Huang X, 2020. Exploring white matter functional networks in children with attention-deficit/hyperactivity disorder. Brain Commun. 2. doi:10.1093/braincomms/fcaa113

Christensen J, Holcomb J, Garver DL, 2004. State-related changes in cerebral white matter may underlie psychosis exacerbation. Psychiatry Res. - Neuroimaging130. doi:10.1016/j.pscychresns.2003.08.002

Cohen J, 2013. Statistical Power Analysis for the Behavioral Sciences, Statistical Power Analysis for the Behavioral Sciences. doi:10.4324/9780203771587

Cohen JD, Barch DM, Carter C, Servan-Schreiber D, 1999. Context-processing deficits in schizophrenia: Converging evidence from three theoretically motivated cognitive tasks. J. Abnorm. Psychol108. doi:10.1037/0021-843X.108.1.120

Cohen JD, Perlstein WM, Braver TS, Nystrom LE, Noll DC, Jonides J, Smith EE, 1997. Temporal dynamics of brain activation during a working memory task. Nature386, 604–608. doi:10.1038/386604a0 [PubMed: 9121583]

Cole MW, Bassett DS, Power JD, Braver TS, Petersen SE, 2014. Intrinsic and task-evoked network architectures of the human brain. Neuron83, 238–251. doi:10.1016/j.neuron.2014.05.014 [PubMed: 24991964]

Cui W, Shang K, Qiu B, Lu J, Gao J-H, 2021. White matter network disorder in mesial temporal epilepsy: An fMRI study. Epilepsy Res. 172, 106590. doi:10.1016/j.eplepsyres.2021.106590 [PubMed: 33639419]

Davis KL, Stewart DG, Friedman JI, Buchsbaum M, Harvey PD, Hof PR, Buxbaum J, Haroutunian V, 2003. White matter changes in schizophrenia evidence for myelin-related dysfunction. Arch. Gen. Psychiatry doi:10.1001/archpsyc.60.5.443

Ding Z, Huang Y, Bailey SK, Gao Y, Cutting LE, Rogers BP, Newton AT, Gore JC, 2018. Detection of synchronous brain activity in white matter tracts at rest and under functional loading. Proc. Natl. Acad. Sci. U. S. A115. doi:10.1073/pnas.1711567115

Driesen NR, Leung H-C, Calhoun VD, Constable RT, Gueorguieva R, Hoffman R, Skudlarski P, Goldman-Rakic PS, Krystal JH, 2008. Impairment of working memory maintenance and response in schizophrenia: functional magnetic resonance imaging evidence. Biol. Psychiatry64, 1026–1034. doi:10.1016/j.biopsych.2008.07.029 [PubMed: 18823880]

Ennaceur A, Neave N, Aggleton JP, 1997. Spontaneous object recognition and object location memory in rats: The effects of lesions in the cingulate cortices, the medial prefrontal cortex, the cingulum bundle and the fornix. Exp. Brain Res113. doi:10.1007/PL00005603

Eryilmaz H, Tanner AS, Ho NF, Nitenson AZ, Silverstein NJ, Petruzzi LJ, Goff DC, Manoach DS, Roffman JL, 2016. Disrupted Working Memory Circuitry in Schizophrenia: Disentangling fMRI Markers of Core Pathology vs Other Aspects of Impaired Performance. Neuropsychopharmacology41, 2411–2420. doi:10.1038/npp.2016.55 [PubMed: 27103065]

Fan Y-S, Li Z, Duan X, Xiao J, Guo X, Han S, Guo J, Yang S, Li J, Cui Q, Liao W, Chen H, 2020. Impaired interactions among white-matter functional networks in antipsychotic-naive first-episode schizophrenia. Hum. Brain Mapp41, 230–240. doi:10.1002/hbm.24801 [PubMed: 31571346]

First MB, Williams JBW, Karg RS, Spitzer RL, Gibbon M, 2008. Structured Clinical interview for DSM-IV Axis I Disorders (SCID-I). Handb. Psychiatr. Meas

Friston KJ, Frith CD, 1995. Schizophrenia: a disconnection syndrome?Clin. Neurosci

Gaffan D, 1994. Dissociated effects of perirhinal cortex ablation, fornix transection and amygdalectomy: evidence for multiple memory systems in the primate temporal lobe. Exp. Brain Res99. doi:10.1007/BF00228977

Gao Y, Li M, Zu Z, Rogers BP, Anderson AW, Ding Z, Gore JC, 2019. Progressive degeneration of white matter functional connectivity in Alzheimer's disease. doi:10.1117/12.2512919

Gao Y, Sengupta A, Li M, Zu Z, Rogers BP, Anderson AW, Ding Z, Gore JC, 2020. Functional connectivity of white matter as a biomarker of cognitive decline in Alzheimer's disease. PLoS One15. doi:10.1371/journal.pone.0240513

Gawryluk JR, Mazerolle EL, D'Arcy RCN, 2014. Does functional MRI detect activation in white matter? A review of emerging evidence, issues, and future directions. Front. Neurosci doi:10.3389/fnins.2014.00239

Gore JC, Li M, Gao Y, Wu TL, Schilling KG, Huang Y, Mishra A, Newton AT, Rogers BP, Chen LM, Anderson AW, Ding Z, 2019. Functional MRI and resting state connectivity in white matter - a mini-review. Magn. Reson. Imaging63. doi:10.1016/j.mri.2019.07.017

Grant DA, Berg E, 1948. A behavioral analysis of degree of reinforcement and ease of shifting to new responses in a Weigl-type card-sorting problem. J. Exp. Psychol38. doi:10.1037/h0059831

Haijma SV, Van Haren N, Cahn W, Koolschijn PCMP, Hulshoff Pol HE, Kahn RS, 2013. Brain volumes in schizophrenia: A meta-analysis in over 18 000 subjects. Schizophr. Bull39. doi:10.1093/schbul/sbs118

Heinrichs RW, Zakzanis KK, 1998. Neurocognitive Deficit in Schizophrenia: A Quantitative Review of the Evidence, Neuropsychology. doi:10.1037//0894-4105.12.3.426

Helenius J, Perkiö J, Soinne L, Østeroaard L, Carano RAD, Salonen O, Savolainen S, Kaste M, Aronen HJ, Tatlisumak T, 2003. Cerebral hemodynamics in a healthy population measured by dynamic susceptibility contrast MR imaging. Acta radiol44. doi:10.1034/j.1600-0455.2003.00104.x

Huang AS, Rogers BP, Anticevic A, Blackford JU, Heckers S, Woodward ND, 2019. Brain function during stages of working memory in schizophrenia and psychotic bipolar disorder. Neuropsychopharmacology44, 2136–2142. doi:10.1038/s41386-019-0434-4 [PubMed: 31185485]

Ji G-J, Ren C, Li Y, Sun J, Liu T, Gao Y, Xue D, Shen L, Cheng W, Zhu C, Tian Y, Hu P, Chen X, Wang K, 2019. Regional and network properties of white matter function in Parkinson's disease. Hum. Brain Mapp40, 1253–1263. doi:10.1002/hbm.24444 [PubMed: 30414340]

Karbasforoushan H, Duffy B, Blackford JU, Woodward ND, 2015. Processing speed impairment in schizophrenia is mediated by white matter integrity. Psychol. Med45, 109–120. doi:10.1017/S0033291714001111 [PubMed: 25066842]

Kay SR, Fiszbein A, Opler LA, 1987. The positive and negative syndrome scale (PANSS) for schizophrenia. Schizophr. Bull13. doi:10.1093/schbul/13.2.261

Kim JJ, Kwon JS, Hae JP, Youn T, Do HK, Myung SK, Dong SL, Myung CL, 2003. Functional disconnection between the prefrontal and parietal cortices during working memory processing in schizophrenia: A [15O]H 2O PET study. Am. J. Psychiatry160. doi:10.1176/appi.ajp.160.5.919

Koshiyama D, Fukunaga M, Okada N, Morita K, Nemoto K, Usui K, Yamamori H, Yasuda Y, Fujimoto M, Kudo N, Azechi H, Watanabe Y, Hashimoto N, Narita H, Kusumi I, Ohi K, Shimada T, Kataoka Y, Yamamoto M, Ozaki N, Okada G, Okamoto Y, Harada K, Matsuo K, Yamasue H, Abe O, Hashimoto Ryuichiro, Takahashi T, Hori T, Nakataki M, Onitsuka T, Holleran L, Jahanshad N, van Erp TGM, Turner J, Donohoe G, Thompson PM, Kasai K, Hashimoto Ryota, COCORO, 2020. White matter microstructural alterations across four major psychiatric disorders: mega-analysis study in 2937 individuals. Mol. Psychiatry25, 883–895. doi:10.1038/s41380-019-0553-7 [PubMed: 31780770]

Kubicki M, Westin CF, Nestor PG, Wible CG, Frumin M, Maier SE, Kikinis R, Jolesz FA, McCarley RW, Shenton ME, 2003. Cingulate fasciculus integrity disruption in schizophrenia: A magnetic resonance diffusion tensor imaging study. Biol. Psychiatry54. doi:10.1016/S0006-3223(03)00419-0

Lancaster JL, Woldorff MG, Parsons LM, Liotti M, Freitas CS, Rainey L, Kochunov PV, Nickerson D, Mikiten SA, Fox PT, 2000. Automated Talairach Atlas labels for functional brain mapping. Hum. Brain Mapp10. doi:10.1002/1097-0193(200007)10:3<120::AID-HBM30>3.0.CO;2-8

Lawrie SM, Buechel C, Whalley HC, Frith CD, Friston KJ, Johnstone EC, 2002. Reduced Frontotemporal Functional Connectivity in Schizophrenia Associated with Auditory Hallucinations, Biol Psychiatry. doi:10.1016/s0006-3223(02)01316-1

Lee J, Park S, 2005. Working memory impairments in schizophrenia: A meta-analysis. J. Abnorm. Psychol doi:10.1037/0021-843X.114.4.599

Lee SH, Kubicki M, Asami T, Seidman LJ, Goldstein JM, Mesholam-Gately RI, McCarley RW, Shenton ME, 2013. Extensive white matter abnormalities in patients with first-episode schizophrenia: A diffusion tensor imaging (DTI) study. Schizophr. Res143, 231–238. doi:10.1016/j.schres.2012.11.029 [PubMed: 23290268]

Lett TA, Voineskos AN, Kennedy JL, Levine B, Daskalakis ZJ, 2014. Treating Working Memory Deficits in Schizophrenia: A Review of the Neurobiology. Biol. Psychiatry75, 361–370. doi:10.1016/j.biopsych.2013.07.026 [PubMed: 24011822]

Levitt JJ, Kubicki M, Nestor PG, Ersner-Hershfield H, Westin CF, Alvarado JL, Kikinis R, Jolesz FA, McCarley RW, Shenton ME, 2010. A diffusion tensor imaging study of the anterior limb of the internal capsule in schizophrenia. Psychiatry Res. - Neuroimaging184. doi:10.1016/j.pscychresns.2010.08.004

Li M, Gao Y, Gao F, Anderson AW, Ding Z, Gore JC, 2020. Functional engagement of white matter in resting-state brain networks. Neuroimage220. doi:10.1016/j.neuroimage.2020.117096

Li M, Newton AT, Anderson AW, Ding Z, Gore JC, 2019. Characterization of the hemodynamic response function in white matter tracts for event-related fMRI. Nat. Commun10. doi:10.1038/s41467-019-09076-2

Lin H, Sun Y, Li M, Zhan Y, Lin L, Ding Z, Han Y, 2020. Sex modulates the apolipoprotein E ε4 effect on white matter and cortical functional connectivity in individuals with amnestic mild cognitive impairment. Eur. J. Neurol27, 1415–1421. doi:10.1111/ene.14226 [PubMed: 32304148]

Logothetis NK, Wandell BA, 2004. Interpreting the BOLD signal. Annu. Rev. Physiol doi:10.1146/annurev.physiol.66.082602.092845

Lynall M-E, Bassett DS, Kerwin R, McKenna PJ, Kitzbichler M, Muller U, Bullmore E, 2010. Functional Connectivity and Brain Networks in Schizophrenia. J. Neurosci30, 9477 LP – 9487. doi:10.1523/JNEUROSCI.0333-10.2010 [PubMed: 20631176]

Manoach DS, Press DZ, Thangaraj V, Searl MM, Goff DC, Halpern E, Saper CB, Warach S, 1999. Schizophrenic subjects activate dorsolateral prefrontal cortex during a working memory task, as measured by fMRI. Biol. Psychiatry doi:10.1016/S0006-3223(98)00318-7

Mazerolle EL, Gawryluk JR, Dillen KNH, Patterson SA, Feindel KW, Beyea SD, Stevens MTR, Newman AJ, Schmidt MH, D'Arcy RCN, 2013. Sensitivity to White Matter fMRI Activation Increases with Field Strength. PLoS One8. doi:10.1371/journal.pone.0058130

Mendrek A, Kiehl KA, Smith A, Irwin D, Forster B, Liddle P, 2005. Dysfunction of a distributed neural circuitry in schizophrenia patients during a working-memory performance. Psychol. Med35, 187–196. doi:10.1017/S0033291704003228 [PubMed: 15841676]

Meyer-Lindenberg AS, Olsen RK, Kohn PD, Brown T, Egan MF, Weinberger DR, Berman KF, 2005. Regionally specific disturbance of dorsolateral prefrontal-hippocampal functional connectivity in schizophrenia. Arch. Gen. Psychiatry62. doi:10.1001/archpsyc.62.4.379

Miyakawa T, Sui R, Deshi M, Suzuki T, Tomonari H, Yasuoka F, rrATETSU S, 1972. Electron Microscopic Study on Schizophrenia Mechanism of Pathological Changes,Acta neuropath. (Berl.). Springer-Verlag.

Nestor PG, Kubicki M, Gurrera RJ, Niznikiewicz M, Frumin M, McCarley RW, Shenton ME, 2004. Neuropsychological correlates of diffusion tensor imaging in schizophrenia. Neuropsychology18, 629–637. doi:10.1037/0894-4105.18.4.629 [PubMed: 15506830]

Oishi K, Faria A, Jiang H, Li X, Akhter K, Zhang J, Hsu JT, Miller MI, van Zijl PCM, Albert M, Lyketsos CG, Woods R, Toga AW, Pike GB, Rosa-Neto P, Evans A, Mazziotta J, Mori S, 2009. Atlas-based whole brain white matter analysis using large deformation diffeomorphic metric mapping: Application to normal elderly and Alzheimer's disease participants. Neuroimage46. doi:10.1016/j.neuroimage.2009.01.002

Paillère-Martinot ML, Caclin A, Artiges E, Poline JB, Joliot M, Mallet L, Recasens C, Attar-Lévy D, Martinot JL, 2001. Cerebral gray and white matter reductions and clinical correlates in patients with early onset schizophrenia. Schizophr. Res50. doi:10.1016/S0920-9964(00)00137-7

Park HJ, Kubicki M, Shenton ME, Guimond A, McCarley RW, Maier SE, Kikinis R, Jolesz FA, Westin CF, 2003. Spatial normalization of diffusion tensor MRI using multiple channels. Neuroimage20. doi:10.1016/j.neuroimage.2003.08.008

Pessoa L, Gutierrez E, Bandettini PA, Ungerleider LG, 2002. Neural Correlates of Visual Working Memory: fMRI Amplitude Predicts Task Performance. Neuron35, 975–987. doi:10.1016/S0896-6273(02)00817-6 [PubMed: 12372290]

Power JD, Barnes KA, Snyder AZ, Schlaggar BL, Petersen SE, 2012. Spurious but systematic correlations in functional connectivity MRI networks arise from subject motion. Neuroimage59, 2142–2154. doi:10.1016/j.neuroimage.2011.10.018 [PubMed: 22019881]

Ramsey NF, Koning HAM, Welles P, Cahn W, van der Linden JA, Kahn RS, 2002. Excessive recruitment of neural systems subserving logical reasoning in schizophrenia. Brain A J. Neurol125, 1793–1807. doi:10.1093/brain/awf188

Rodrigue AL, Schaeffer DJ, Pierce JE, Clementz BA, McDowell JE, 2018. Evaluating the Specificity of Cognitive Control Deficits in Schizophrenia Using Antisaccades, Functional Magnetic Resonance Imaging, and Healthy Individuals With Poor Cognitive Control . Front. Psychiatry doi:10.3389/fpsyt.2018.00107

Rosenberger G, Nestor PG, Oh JS, Levitt JJ, Kindleman G, Bouix S, Fitzsimmons J, Niznikiewicz M, Westin CF, Kikinis R, McCarley RW, Shenton ME, Kubicki M, 2012. Anterior limb of the internal capsule in schizophrenia: A diffusion tensor tractography study. Brain Imaging Behav. 6. doi:10.1007/s11682-012-9152-9

Rosvold HE, Mirsky AF, Sarason I, Bransome ED, Beck LH, 1956. A continuous performance test of brain damage. J. Consult. Psychol20. doi:10.1037/h0043220

Rottschy C, Langner R, Dogan I, Reetz K, Laird AR, Schulz JB, Fox PT, Eickhoff SB, 2012. Modelling neural correlates of working memory: A coordinate-based meta-analysis. Neuroimage60, 830–846. doi:10.1016/j.neuroimage.2011.11.050 [PubMed: 22178808]

Ruíz DSM, Yilmaz H, Gailloud P, 2009. Cerebral developmental venous anomalies: Current concepts. Ann. Neurol doi:10.1002/ana.21754

Schilling K, Gao Y, Janve V, Stepniewska I, Landman BAA, Anderson AWW, 2018. Confirmation of a gyral bias in diffusion MRI fiber tractography. Hum. Brain Mapp39. doi:10.1002/hbm.23936

Schmahmann JD, Pandya DN, 2009. Fiber Pathways of the Brain, Fiber Pathways of the Brain. doi:10.1093/acprof:oso/9780195104233.001.0001

Sigmundsson T, Suckling J, Maier M, Williams SCR, Bullmore ET, Greenwood KE, Fukuda R, Ron MA, Toone BK, 2001. Structural abnormalities in frontal, temporal, and limbic regions and

interconnecting white matter tracts in schizophrenic patients with prominent negative symptoms. Am. J. Psychiatry158. doi:10.1176/appi.ajp.158.2.234

Skudlarski P, Schretlen DJ, Thaker GK, Stevens MC, Keshavan MS, Sweeney JA, Tamminga CA, Clementz BA, O'Neil K, Pearlson GD, 2013. Diffusion tensor imaging white matter endophenotypes in patients with schizophrenia or psychotic bipolar disorder and their relatives. Am. J. Psychiatry170. doi:10.1176/appi.ajp.2013.12111448

Theilmann RJ, Reed JD, Song DD, Huang MX, Lee RR, Litvan I, Harrington DL, 2013. White-matter changes correlate with cognitive functioning in Parkinson's disease. Front. Neurol4, 37. doi:10.3389/fneur.2013.00037 [PubMed: 23630517]

Thermenos HW, Goldstein JM, Buka SL, Poldrack RA, Koch JK, Tsuang MT, Seidman LJ, 2005. The effect of working memory performance on functional MRI in schizophrenia. Schizophr. Res74, 179–194. doi:10.1016/j.schres.2004.07.021 [PubMed: 15721998]

Tomasi D, Volkow ND, 2010. Functional connectivity density mapping. Proc. Natl. Acad. Sci. U. S. A107, 9885–9890. doi:10.1073/pnas.1001414107 [PubMed: 20457896]

Tourjman SV, Juster RP, Purdon S, Stip E, Kouassi E, Potvin S, 2019. The screen for cognitive impairment in psychiatry (SCIP) is associated with disease severity and cognitive complaints in major depression. Int. J. Psychiatry Clin. Pract23. doi:10.1080/13651501.2018.1450512

Van Snellenberg JX, Torres IJ, Thornton AE, 2006. Functional neuroimaging of working memory in schizophrenia: task performance as a moderating variable. Neuropsychology20, 497–510. doi:10.1037/0894-4105.20.5.497 [PubMed: 16938013]

Venegas J, Clark E, 2011. Wechsler Test of Adult Reading, in: Kreutzer JS, DeLuca J, Caplan B (), Encyclopedia of Clinical Neuropsychology. Springer New York, New York, NY, pp. 2693–2694. doi:10.1007/978-0-387-79948-3_1500

Venkataraman A, Whitford TJ, Westin CF, Golland P, Kubicki M, 2012. Whole brain resting state functional connectivity abnormalities in schizophrenia. Schizophr. Res139. doi:10.1016/j.schres.2012.04.021

Wechsler D, 1945. A Standardized Memory Scale for Clinical Use. J. Psychol. Interdiscip. Appl19. doi:10.1080/00223980.1945.9917223

Wiser AK, Andreasen NC, O'Leary DS, Watkins GL, Boles Ponto LL, Hichwa RD, 1998. Dysfunctional cortico-cerebellar circuits cause "cognitive dysmetria" in schizophrenia. Neuroreport9. doi:10.1097/00001756-199806010-00042

Woodward ND, Heckers S, 2016. Mapping Thalamocortical Functional Connectivity in Chronic and Early Stages of Psychotic Disorders. Biol. Psychiatry79, 1016–1025. doi:10.1016/j.biopsych.2015.06.026 [PubMed: 26248537]

Wu T-L, Wang F, Li M, Schilling KG, Gao Y, Anderson AW, Chen LM, Ding Z, Gore JC, 2019. Resting-state white matter-cortical connectivity in non-human primate brain. Neuroimage184. doi:10.1016/j.neuroimage.2018.09.021

Wu TL, Wang F, Anderson AW, Chen LM, Ding Z, Gore JC, 2016. Effects of anesthesia on resting state BOLD signals in white matter of non-human primates. Magn. Reson. Imaging34. doi:10.1016/j.mri.2016.07.001

Yang C, Zhang W, Yao L, Liu N, Shah C, Zeng J, Yang Z, Gong Q, Lui S, 2020. Functional Alterations of White Matter in Chronic Never-Treated and Treated Schizophrenia Patients. J. Magn. Reson. Imaging52, 752–763. doi:10.1002/jmri.27028 [PubMed: 31859423]

Yeganeh-Doost P, Gruber O, Falkai P, Schmitt A, 2011. The role of the cerebellum in schizophrenia: From cognition to molecular pathways. Clinics66. doi:10.1590/S1807-59322011001300009

Zhou SY, Suzuki M, Hagino H, Takahashi T, Kawasaki Y, Nohara S, Yamashita I, Seto H, Kurachi M, 2003. Decreased volume and increased asymmetry of the anterior limb of the internal capsule in patients with schizophrenia. Biol. Psychiatry54. doi:10.1016/S0006-3223(03)00007-6

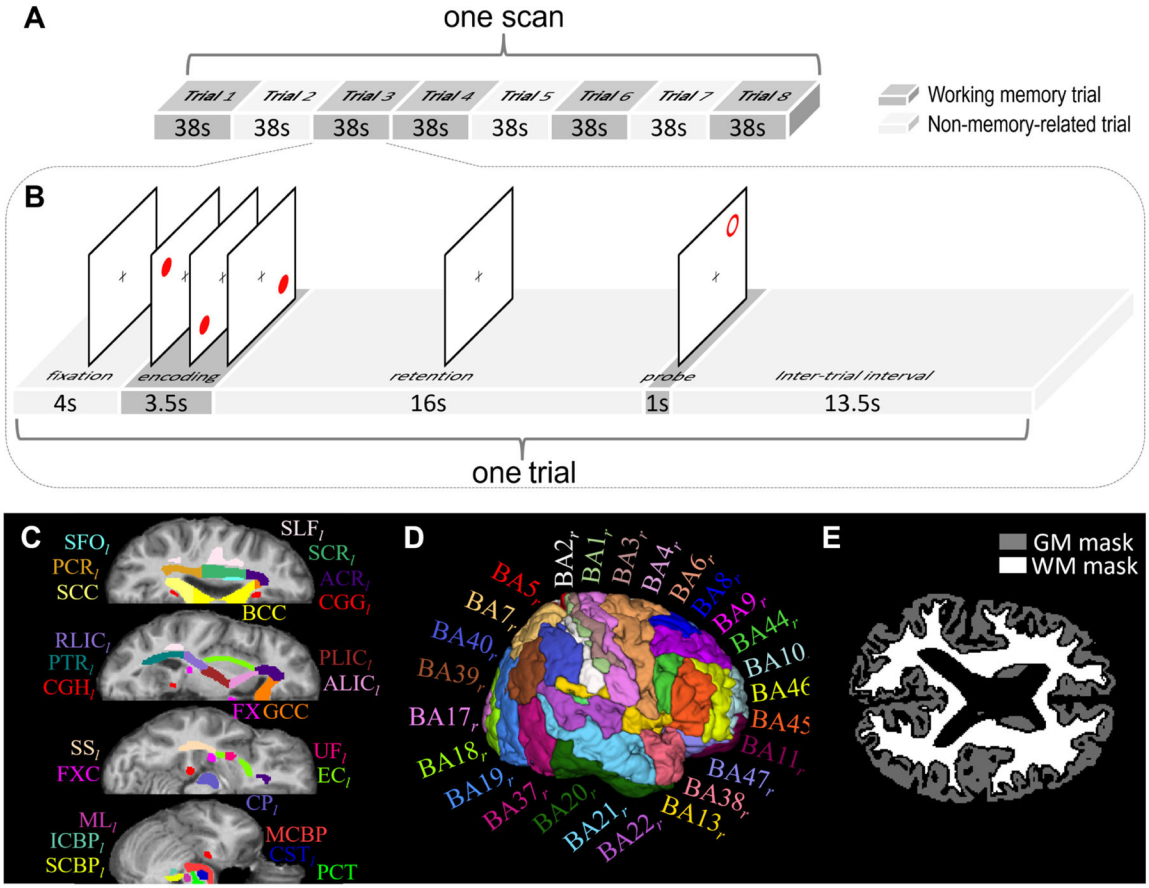

Fig. 1.

Schematic diagram of spatial working memory task, atlases of white matter (WM)/gray matter (GM) ROIs, and tissue masks. **(A)** One task scan comprised eight trials, of which five were memory trials (dark gray blocks) and the other three were non-memory trials (light gray blocks). **(B)** Each memory trial lasted 38s, including 4s of fixation, 3.5s of encoding, 16s of retention, 1s of probe and 13.5s of interval. The non-memory trial had the same sequence of events, except that the subjects were instructed not to remember the target locations. **(C)** WM parcellation atlas and **(D)** GM parcellation atlas in MNI space were used to initially define WM and GM ROIs. See Table 2 for the lists of these ROIs. **(E)** Whole-brain WM and GM tissue masks of one subject that were used to further constrain WM and GM ROIs to avoid partial volume effect.

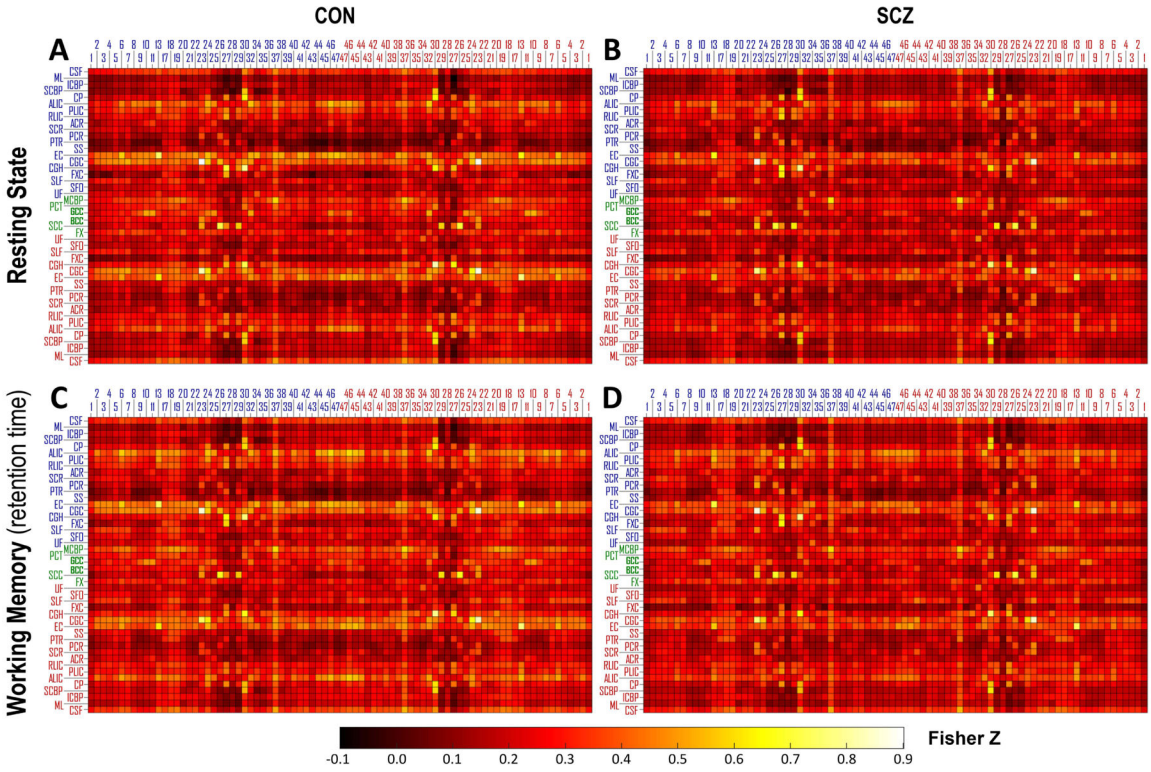

Fig. 2.

Group mean of functional correlation matrix (mFCM) within CON group and SCZ group under two conditions: **(A**, **B)** resting state and **(C, D)** retention period during the spatial working memory task. The blue/red numbers labeling columns of mFCM indicate the indices of Brodmann area (BA) in left/right hemisphere. The blue/green/red abbreviations labeling rows of mFCM indicate the WM bundles in left/middle/right portion of brain. See Table 2 for the lists of these ROIs.

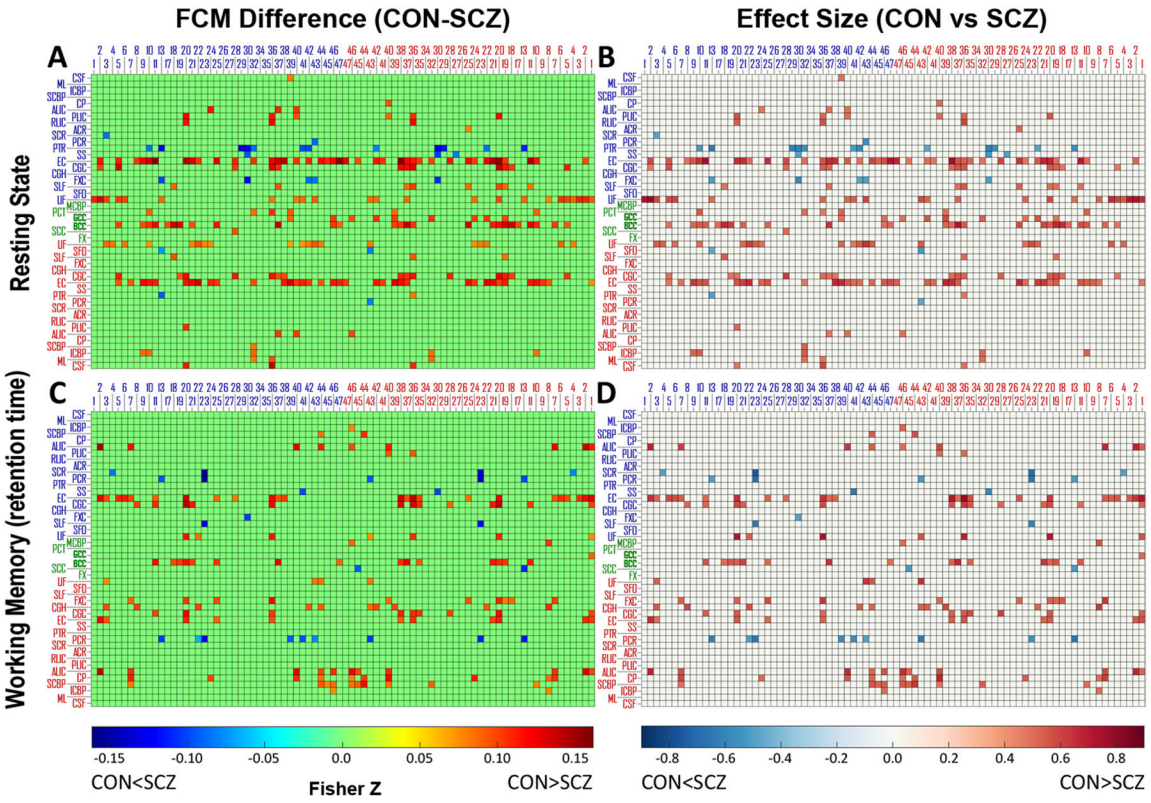

Fig. 3.

Differences and effect sizes of FCM between CON group and SCZ group under two conditions. Difference of subtracting mFCM of SCZ from mFCM of CON and effect size of the difference under two conditions: **(A, B)** resting state and **(C, D)** working memory task. The differences of FCM elements with $p_{FDR}>0.05$ were set to zero and the corresponding effect sizes were also set to zero. The blue/red numbers labeling columns indicate indices of Brodmann areas in left/right hemisphere. The blue/green/red abbreviations labeling rows indicate WM bundles in left/middle/right portion of brain. See Table 2 for the lists of these ROIs.

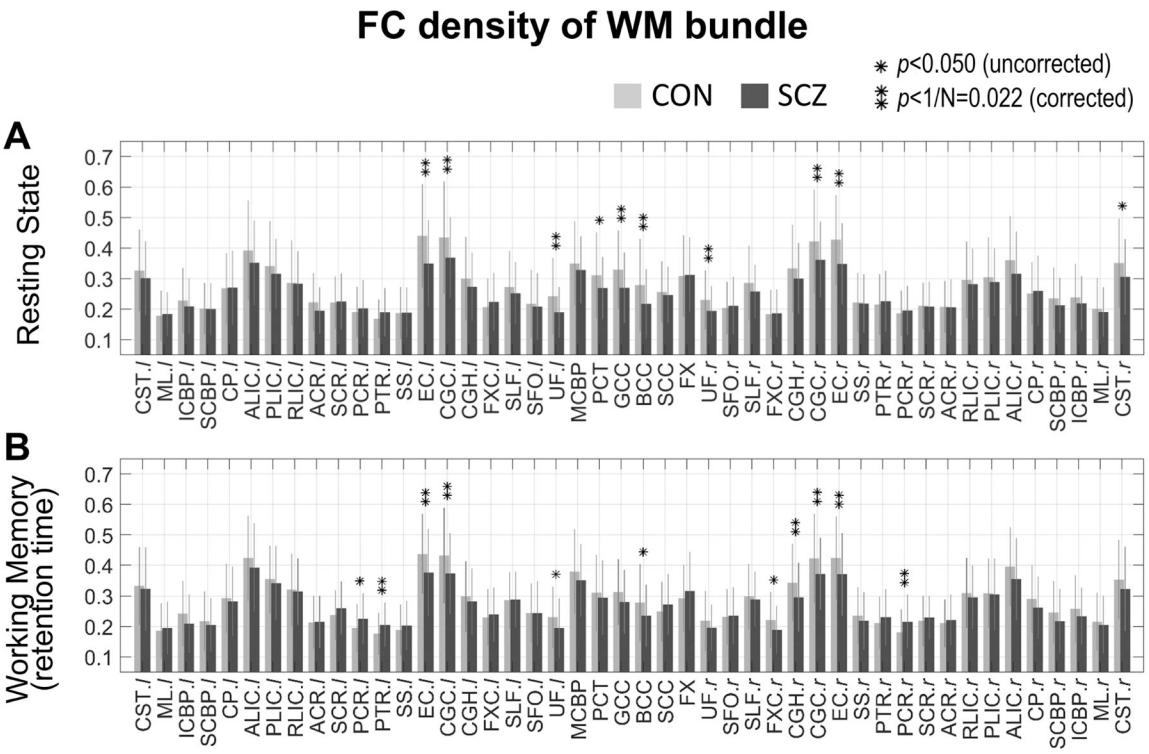

Fig. 4.

Comparison of WM FC density between CON group and SCZ group under two conditions. Mean and standard deviation of FC density within CON group (light gray bar and error bar) and SCZ group (dark gray bar and error bar) under two conditions: **(A)** resting state and **(B)** working memory task. * indicates $p<0.05$ (uncorrected significance level) and ** indicates $p<1/N=0.022$ (corrected significance level). See Supplementary Table 1 for a summary of group mean, standard deviation and p-values of each WM bundle.

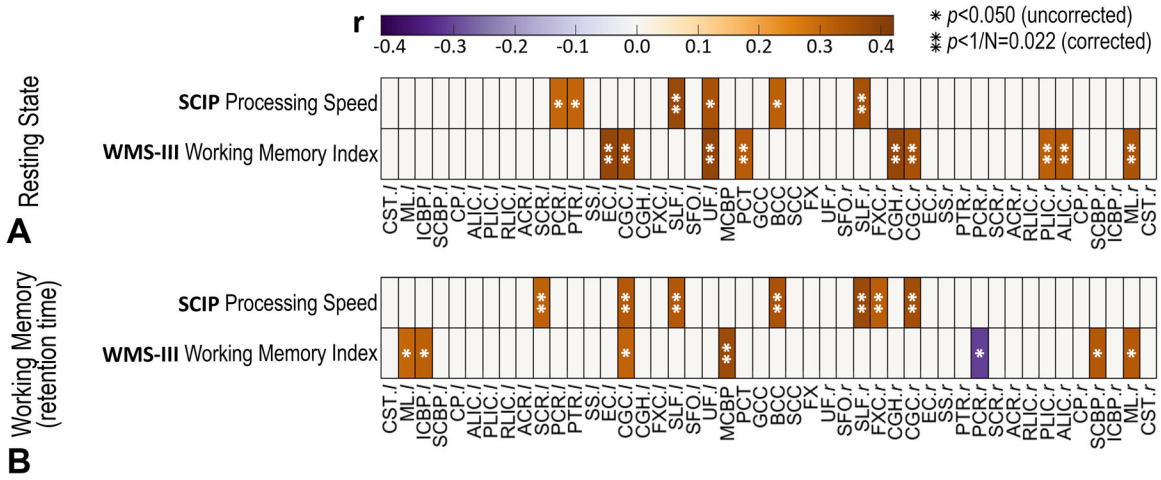

Fig. 5.

Correlation coefficients between FC and cognitive scores under two conditions: **(A)** resting state and **(B)** working memory task. Given one WM bundle and one score, the correlation coefficient shown here is the one with maximum amplitude among all 82 correlation coefficients between the score and 82 FC that the WM bundle corresponds to. All the coefficients with $|r|<0.3$ or $p>0.05$ are set to zero. * indicates $p<0.05$ (uncorrected significance level) and ** indicates $p<1/N=0.022$ (corrected significance level).

Table 1.

Demographics, clinical and cognitive characteristics

	CON	SCZ	Statistics	
	***n*=67**	***n*=84**	t/χ^2	***p***
Sex [male:female]	41:26	57:27	0.73	0.394
Race [W:AA:O]	48:13:6	55:27:2	5.53	0.063
Handedness [R:L]	60:7	77:7	0.20	0.656
	Mean±SD	**Mean±SD**		
Age [years]	28.8±9.1	27.3±9.4	1.04	0.302
Maternal education [years]	14.6±2.4	14.6±2.7	−0.16	0.874
Paternal education [years]	15.1±2.8	14.8±3.6	0.57	0.571
Illness duration [months]	-	76.9±97.1	-	-
Antipsychotic dosage (Chlorpromazine equivalents)	-	368.0±220.4	-	-
PANSS Positive	-	15.8±8.8	-	-
PANSS Negative	-	14.3±5.4	-	-
PANSS General	-	28.7±8.1	-	-
WTAR Premorbid IQ	107.9±15.0	102.1±9.5	2.93	0.004
WMS-III Working Memory Index	106.7±12.4	94.8±11.0	6.25	<0.001
SCIP Verbal Leaning-Immediate z-score	0.39±0.88	−0.86±1.26	6.88	<0.001
SCIP Verbal Leaning-Delayed z-score	0.17±0.97	−0.83±1.20	5.54	<0.001
SCIP Working Memory z-score	0.32±0.97	−0.70±1.32	5.32	<0.001
SCIP Verbal Fluency z-score	0.64±1.04	−0.10±1.10	4.19	<0.001
SCIP Processing Speed z-score	−0.20±1.05	−1.59±1.06	7.99	<0.001
SCIP Global Cognition z-score	0.26±0.59	−0.81±0.76	9.54	<0.001
AX-CPT d'-Context	3.6±0.7	2.7±1.0	5.92	<0.001
WCST Total Correct	52.4±6.5	45.7±11.4	4.18	<0.001
tfMRI Total Correct Number	25.1±3.8	22.5±5.6	3.20	0.002
tfMRI Total Response Time [ms]	1085.7±381.3	1306.0±591.0	−2.64	0.009

W-white; AA-African American; O-others; WTAR-Wechsler Test of Adult Reading; PANSS-Positive and Negative Syndrome Scale; WMS-III: Wechsler Memory Scale, third version; SCIP-Screen for Cognitive Impairment in Psychiatry; AX-CPT-AX Continuous Performance Task; WCST-Wisconsin Card Sorting Test.

Table 2.

List of white matter and gray matter ROIs (BA: Brodmann area).

White Matter (WM) ROIs	Gray Matter (GM) ROIs
CST: Corticospinal Tract	BA1: Primary Somatosensory Cortex 1
ML: Medial Lemniscus	BA2: Primary Somatosensory Cortex 2
ICBP: Inferior Cerebellar Peduncle	BA3: Primary Somatosensory Cortex 3
SCBP: Superior Cerebellar Peduncle	BA4: Primary Motor Cortex
CP: Cerebral Peduncle	BA5: Somatosensory Association Cortex
ALIC: Anterior Limb of Internal Capsule	BA6: Premotor and Supplementary Motor
PLIC: Posterior Limb of Internal Capsule	BA7: Visuo-Motor Coordination
RLIC: Retrolenticular Limb of Internal Capsule	BA8: Frontal Eye Fields
ACR: Anterior Corona Radiata	BA9: Dorsolateral Prefrontal Cortex
SCR: Superior Corona Radiata	BA10: Anterior Prefrontal Cortex
PCR: Posterior Corona Radiata	BA11: Orbitofrontal Area
PTR: Posterior Thalamic Radiation (include Optic Radiation)	BA13: Insular Cortex
SS: Sagittal Stratum (include inferior longitudinal fasciculus and fronto-occipital fasciculus)	BA17: Primary Visual Cortex (V1)
EC: External Capsule	BA18: Secondary Visual Cortex (V2)
CGC: Cingulum (Cingulate Gyrus)	BA19: Associative Visual Cortex (V3–5)
CGH: Cingulum (Hippocampus)	BA20: Inferior Temporal Gyrus
FXC: Fornix (Cres)	BA21: Middle Temporal Gyrus
SLF: Superior Longitudinal Fasciculus	BA22: Superior Temporal Gyrus
SFO: Superior Fronto-Occipital Fasciculus	BA23: Ventral Posterior Cingulate Cortex
UF: Uncinate Fasciculus	BA24: Ventral Anterior Cingulate Cortex
MCBP: Middle Cerebellar Peduncle	BA25: Subgenual Area
PCT: Pontine Crossing Tract	BA26: Ectosplenial Portion of Retrosplenial Region
GCC: Genu of Corpus Callosum	BA27: Piriform Cortex
BCC: Body of Corpus Callosum	BA28: Ventral Entorhinal Cortex
SCC: Splenium of Corpus Callosum	BA29: Retrosplenial Cingulate Cortex
FX: Fornix	BA30: Part of Cingulate Cortex
	BA32: Dorsal Anterior Cingulate Cortex
	BA34: Dorsal Entorhinal Cortex
	BA35: Perirhinal Cortex
	BA36: Ectorhinal Area
	BA37: Occipitotemporal Area (part of fusiform gyrus and interior temporal gyrus
	BA38: Temporopolar Area
	BA39: Angular Gyrus
	BA40: Supramarginal Gyrus
	BA41: Auditory Cortex 1
	BA42: Auditory Cortex 2
	BA43: Primary Gustatory Cortex
	BA44: Pars Opercularis
	BA45: Pars Triangularis

White Matter (WM) ROIs	Gray Matter (GM) ROIs
	BA46: Dorsolateral Prefrontal Cortex BA47: Pars Orbitalis